



**Table I.** Computed Energies, Number of Negative Force Constants ( $k < 0$ ), Geometries, Dipole Moments, and Zero-Point Energies (ZPE's) for  $\text{NH}_2\text{NO}_2$  Structures<sup>a</sup>

	HF/3-21G	HF/6-31G*	MP2/6-31G*
<b>III, <math>C_{2v}</math></b>			
$E_{\text{tot}}$ (au)	-258.13794	-259.63645	-260.34700
no. of $k < 0$	0	1	
$E_{\text{rel}}$ (kcal)	0.0	0.0	0.0
$R(\text{N-N})$	1.355	1.327	1.361
$R(\text{N-O})$	1.247	1.194	1.235
$\angle\text{NNO}$	116.4	116.6	116.2
$\angle(\text{N-H})$	0.995	0.992	1.008
$\angle\text{NNH}$	116.0	116.7	116.6
$\mu$	4.66	4.54	4.13
ZPE (kcal)	24.22	26.43	
<b>IV, <math>C_s</math></b>			
$E_{\text{tot}}$ (au)		-259.63941	-260.35192
$E_{\text{rel}}$ (kcal)		-1.86	-3.09
$R(\text{N-N})$		1.356 (1.381, <sup>b</sup> 1.427 <sup>c</sup> )	1.398
$R(\text{N-O})$		1.191 (1.232, <sup>b</sup> 1.206 <sup>c</sup> )	1.233
$\angle\text{ONO}$		127.0 (132.7, <sup>b</sup> 130.1 <sup>c</sup> )	127.6
$\alpha$		177.9	176.3
$R(\text{N-H})$		0.998 (1.007, <sup>b</sup> 1.005 <sup>c</sup> )	1.017
$\angle\text{HNNH}$		116.8 (120.9, <sup>b</sup> 115.2 <sup>c</sup> )	114.4
$\beta$		48.0 (46.9, <sup>b</sup> 51.8 <sup>c</sup> )	54.5
$\mu$		4.17	3.65
ZPE (kcal)		27.40	
<b>V, <math>C_{2v}</math></b>			
$E_{\text{tot}}$ (au)	-258.10811	-259.60124	-260.31651
no. of $k < 0$	2	2	
$E_{\text{rel}}$ (kcal)	18.7	22.1	19.1
$R(\text{N-N})$	1.423	1.386	1.406
$R(\text{N-O})$	1.234	1.188	1.238
$\angle\text{NNO}$	117.0	117.1	117.0
$R(\text{N-H})$	0.994	0.991	1.004
$\angle\text{NNH}$	116.4	117.0	117.4
$\mu$	3.96	3.78	3.26
ZPE (kcal)	23.45	25.50	
<b>VI, <math>C_s</math></b>			
$E_{\text{tot}}$ (au)	-258.11831	-259.61983	-260.33583
no. of $k < 0$	1	1	
$E_{\text{rel}}$ (kcal)	12.3	10.4	7.0
$R(\text{N-N})$	1.473	1.421	1.462
$R(\text{N-O})$	1.219	1.178	1.228
$\angle\text{NNO}$	116.3	116.0	115.3
$R(\text{N-O})$	1.243	1.193	1.235
$\angle\text{NNO}$	116.4	117.2	117.4
$R(\text{N-H})$	1.012	1.005	1.024
$\angle\text{NNH}$	104.9	104.4	102.9
$\beta$	63.2	65.1	68.7
$\mu$	3.62	3.43	2.91
ZPE (kcal)	24.5	26.90	

<sup>a</sup> Experimental parameters shown in parentheses. Energies as indicated, bond lengths in Å, angles in deg, dipole moment in D. <sup>b</sup> Reference 8. <sup>c</sup> Reference 3.

The calculated geometry for IV shows that not only is the  $\text{NH}_2$  nitrogen pyramidal, the  $\text{NO}_2$  nitrogen is also. A similar feature has been observed for nitromethane, both experimentally and theoretically.<sup>9</sup> As indicated for IV, the nitrogens are pyramidalized in opposite directions. This might be interpreted as minimizing electron repulsions between the amino lone pair and the  $\pi$  system of the nitro group. Cyanamide and ethynamine are also observed to possess a pyramidal  $\text{NH}_2$  group and nonlinear  $\text{N}-\text{C}\equiv\text{X}$ :  $\text{X} = \text{N}$ ,  $\text{C}-\text{H}$  linkages.<sup>10</sup> Thus, nitramide, cyanamide, and ethynamine show similar deviations from idealized models based on resonance interactions.

The calculations show that the preference for the pyramidal geometry in nitramide is not large. Substitution can change this preference and dimethylnitramine (I,  $\text{R}_1 = \text{R}_2 = \text{CH}_3$ ), for ex-

**Table II.** Atom Equivalents and Derived Energies (in au) Used To Calculate the  $\Delta H_f^\circ$  (in kcal/mol) of Nitramide

atom equiv	3-21G	6-31G*
2H(N)	2(-0.56322)	2(-0.5636)
N(H) <sub>2</sub> (C)	-54.16469	-54.46869
$\text{NO}_2$	-202.84670	-24.03509
sum	-258.13783	-259.63650
$E_{\text{tot}}$	-258.13794	-259.63941
$\Delta H_f^\circ$	-0.1 kcal	-1.8 kcal

**Table III.** Calculated Atomic Populations at HF/6-31G\*<sup>a</sup>

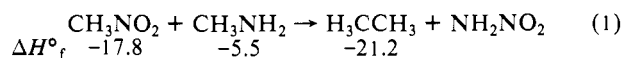
	III	IV	V	VI
$\text{N}_1$	7.780	7.721	7.827	7.662
$\text{N}_2$	6.167	6.161	6.163	6.180
$\text{O}_3$	8.539	8.531	8.504	8.480
$\text{O}_4$	8.539	8.531	8.504	8.540
H	0.491	0.525	0.501	0.565

<sup>a</sup> Individual populations are believed to be  $\pm 0.005$  e. The sum reflects only slightly less precision due to cancellation of errors.

ample, has a planar amine nitrogen in the gas phase and the high-temperature crystal phase.<sup>11</sup> Nonetheless, pyramidalization at the amine nitrogen in dimethylnitramine is detectable in its low-temperature crystalline form.<sup>11b</sup> Also, the X-ray data indicate that nitramide probably has a planar geometry in the solid phase.<sup>12</sup> Thus, the preference for pyramidal or planar configuration is sufficiently small that crystal forces can alter geometries from those observed in the gas phase.

Without consideration of ZPE, inversion barriers of 1.9 and 3.1 kcal/mol are found at HF/6-31G\* and MP2/6-31G\*, respectively. Vibrational frequencies and thus ZPE's calculated at HF/6-31G\* are typically about 10% too high.<sup>13</sup> Appropriate scaling of the ZPE values found in Table I leads to a corrected ZPE difference between III and IV of -0.9 kcal/mol, yielding finally an inversion barrier of 1.0 kcal at HF/6-31G\* and 2.2 kcal at MP2/6-31G\*. The latter value compares with experimental estimate of 2.7 kcal/mol.<sup>14</sup> Further comparisons are observed barriers of 5.8 kcal/mol for ammonia<sup>15</sup> and 4.8 kcal/mol for methylamine.<sup>16</sup>

To determine what thermodynamic stabilization may result from involvement of II, estimates of the heat of formation of nitramide can be made from the calculated total energies and the atom equivalents of Ibrahim and Schleyer.<sup>17</sup> Resonance stabilization, if it exists, can then be detected as the difference between the  $\Delta H_f^\circ$  from the ab initio calculations and simple models assuming group additivity. Results using the ab initio calculations are shown in Table II and are in good agreement with a previous calculation by different means of -0.77 kcal/mol.<sup>6a</sup> Equation 1 shows a simple reaction and observed heats of formation<sup>18</sup> which, if simple group additivity holds, represents a nitramide  $\Delta H_f^\circ$  without resonance stabilization. Comparison of the results shows that the  $\Delta H_f^\circ$  obtained from the HF/6-31G\* calculation of -1.8 kcal is nearly the same as that from eq 1, -2.1 kcal. Thus, resonance stabilization is calculated to be less than 1 kcal/mol.



$$\Delta H_f^\circ \text{ for } \text{NH}_2\text{NO}_2 = -2.1 \text{ kcal assuming } \Delta H_f^\circ = 0.0$$

(11) (a) Stolevik, R.; Rademacher, P. *Acta Chem. Scand.* **1969**, *23*, 672. (b) Filhol, A.; Bravic, G.; Rey-Lafon, M.; Thomas, M. *Acta Crystallogr.* **1980**, *36B*, 575. (c) Krebs, B.; Mandt, J.; Cobbleddick, R. E.; Small, R. W. H. *Acta Crystallogr.* **1979**, *35B*, 402.

(12) Beevers, G. H.; Trotman-Dickenson, A. F. *Acta Crystallogr.* **1957**, *10*, 34.

(13) Hehre, W. J.; Radom, L.; Schleyer, P. v. R.; Pople, J. A. *Ab Initio Molecular Orbital Theory*; Wiley: New York, 1986; pp 226-261.

(14) Lister, D. G.; Tyler, J. K. *Chem. Commun.* **1966**, 152.

(15) Swalen, J. D.; Ibers, J. A. *J. Chem. Phys.* **1962**, *36*, 1914.

(16) Tsuboi, M.; Hirakawa, A. Y.; Tamagake, K. *J. Mol. Spectrosc.* **1967**, *22*, 272.

(17) Ibrahim, M. R.; Schleyer, P. v. R. *J. Comput. Chem.* **1985**, *6*, 157.

(18) Pedley, J. B.; Naylor, R. D.; Kirby, S. P. *Thermochemical Data of Organic Compounds*, 2nd ed.; Chapman and Hall: New York, 1986.

(9) Bock, C. W.; Krasnoshchiokov, S. V.; Khristenko, L. V.; Panchenko, U. N.; Pentin, Y. A. *J. Mol. Struct. (Theochem.)* **1987**, *149* (34), 201 and references therein.

(10) Saebo, S.; Farnell, N. V.; Radom, L. *J. Am. Chem. Soc.* **1984**, *106*, 5047.

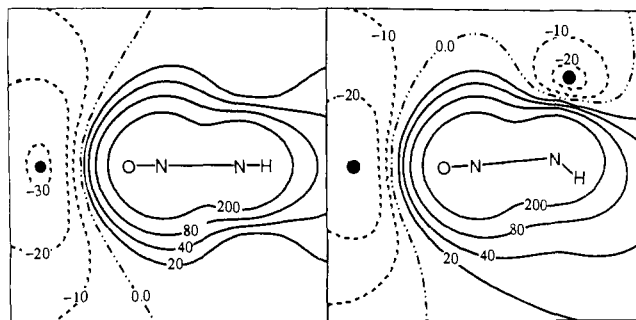


**Figure 1.** Calculated electrostatic potential at HF/6-31G\*/HF/6-31G\* in kcal mol<sup>-1</sup> e<sup>-1</sup> for planar (left) and pyramidal (right) nitramide. Potentials shown in the symmetry plane; minima are indicated with a filled circle. In the left-hand panel, the minimum associated with the nitro oxygens is -32 kcal mol<sup>-1</sup> e<sup>-1</sup>. In the right-hand panel, minimum associated with the amine lone pair is -23 kcal mol<sup>-1</sup> e<sup>-1</sup> and the minimum associated with the nitro oxygens is -29 kcal mol<sup>-1</sup> e<sup>-1</sup>.

The above argument aside, one could reasonably state that the resonance stabilization energy from II could not exceed the difference in the inversion barriers between ammonia (5.8 kcal/mol) and nitramide (2.7 kcal/mol) of about 3 kcal/mol, otherwise the molecule would be planar. The paragraph above simply suggests that the contribution is even smaller than this. In a related case, the resonance stabilization energy found for *p*-nitroaniline has not been detected experimentally.<sup>19</sup>

Additional data inconsistent with extensive involvement of II are the calculated geometries of III–VI. Significant contributions from II should lead to shorter N–N bonds accompanied by longer N–O bonds when resonance delocalization onto the nitro group is possible. At the most accurate level of theory, MP2/6-31G\*, it is found that the N–O bond lengths in III–VI are remarkably similar at about 1.235 ± 0.003, even in cases where no nitro group amine lone pair resonance is possible. The only exception, the NO bond eclipsing the amine lone pair in VI, may be unusually short because of repulsions between oxygen and amine nitrogen lone pairs. This near constant value of the N–O bond length is found despite larger variations in the N–N bond length. The N–N bond length variations cannot be uniquely attributed to increased  $\pi$  character in the bond, as the change in hybridization at the amine will also cause shortening of this distance, as demonstrated by the N–N distance difference in V and VI.

Atomic populations obtained by integration over virial fragments<sup>20</sup> at HF/6-31G\* are shown in Table II. The HF/6-31G\* level provides results qualitatively similar to those at MP2/6-31G\*, and use of the lower level of theory is not expected to lead to significant quantitative errors. Nevertheless, the dipole moment is overestimated at the HF level while the MP2 dipole moment for nitramide of 3.65 D is in very good agreement with the observed value of 3.78 D.<sup>21</sup> Structure II indicates the transfer of charge from the amino N to the nitro group, but the integration shows that the population of that atom increases as the center becomes planar. There is a net transfer of charge from the NH<sub>2</sub> moiety to the NO<sub>2</sub> moiety as II becomes planar, as indicated by the total group populations; thus the dipole moment increases on going from IV to III. Inspection of Table II reveals that additional charge on the nitro group in III comes from the hydrogens. A similar effect is found in comparing V and VI. Thus, the increased dipole moments calculated for IV → III and VI → V cannot be simply rationalized as resulting from increased importance of II.

The electrostatic potentials of III and IV, shown in Figure 1, provide additional information concerning the participation of II. As shown previously,<sup>2,68</sup> in the planar configuration there are no

negative potentials associated with the amine nitrogen. IV, however, exhibits the expected negative potentials over the amine nitrogen resulting from its lone pair of electrons. Thus, despite a lesser total charge for the amine nitrogen found in IV than III, the anisotropic nature of the amine lone pair gives rise to the usual negative potentials. The magnitude of the minimum of the potential in this region is, however, significantly reduced from that found for ammonia, but slightly larger than that found in formamide.<sup>22</sup> Precise comparisons are difficult due to differences in basis set.

The calculated rotational barrier for nitramide, found at HF/6-31G\* and MP2/6-31G\* as the energy difference between IV and VI, without ZPE differences is 12.3 and 10.1 kcal/mol, respectively. ZPE differences are only a few tenths of a kilocalorie and thus negligible. A barrier obtained at HF/3-21G as the energy difference between III and IV is 12.3 kcal/mol—nearly the same as that found at the higher levels of theory. The size of the barrier is intermediate between those found in gaseous nitrobenzenes of 2.8–3.3 kcal/mol<sup>23</sup> and those found for formamide in solution of 17–21 kcal/mol.<sup>24</sup> The calculated barrier should be quite reliable. Direct comparison with experiment is not possible, due to a lack of experimental data. Rotational barriers for dimethylamine, however, are 12 kcal/mol from INDO calculations<sup>25</sup> and >9 kcal/mol estimated experimentally.<sup>26</sup>

If the resonance stabilization of nitramide is only a kilocalorie or so, what then causes the rotational barrier of 10–12 kcal/mol? Several calculated properties suggest that unfavorable dipole-dipole interaction between the N–O bond and amine lone pair as well as increased electron–electron repulsions between the oxygen lone pair and amine lone pair in the transition state give rise to the calculated rotational barrier. Thus, the increased rotational barrier over that found in nitromethane (6.0 cal/mol in the gas phase)<sup>27</sup> results from a combination of a decrease in the degeneracy of the rotational cycle (from 6-fold to 2-fold), the greater repulsion energy of lone pair–lone pair interactions over the oxygen lone pair–CH bonded pair, and less favorable dipole–dipole interactions. The increased repulsions and unfavorable dipole interactions are evidenced by the geometrical and charge distribution differences between IV and VI. The N–N bond is lengthened and charge is displaced from the oxygen eclipsing the amine lone pair, resulting in a short N–O<sub>3</sub> bond distance.

Wiberg and Laidig questioned the importance of resonance interactions in amides.<sup>56</sup> They find little change in the CO bond length with rotation about the C–N bond in formamide. Similarly, in nitramide, the NO bond length is relatively insensitive to configuration about the amine. Also, the charge obtained from integration over the nitrogen basin in planar formamide exceeds that found in the rotated geometries with pyramidal nitrogens. Despite these similarities, nitramide has a pyramidal nitrogen, while formamide has a planar nitrogen, albeit one that is easily distorted.<sup>5b</sup> The NH<sub>2</sub> rotational barrier in formamide is also significantly larger than that in nitramide. Thus the question arises as to what causes these differences.

Reviews of inversion at nitrogen are available.<sup>4a,26</sup> Important factors are found to be electronegativity of the attached atom or group and  $\pi$  conjugation. Increased electronegativity of a substituent favors a pyramidal nitrogen while  $\pi$  conjugation favors a planar nitrogen.

Dominant contributions from  $\pi$  configuration in determining the configuration at nitrogen suggests the pyramidal-planar energy difference might be correlated with linear free energy (lfe) pa-

(22) Scrocco, E.; Tomasi, J. *Top. Curr. Chem.* **1973**, *42*, 95.

(23) (a) Høg, J. H.; Nygaard, L.; Sorensen, G. O. *J. Mol. Struct.* **1971**, *7*, 111. (b) Correll, T.; Larsen, N. W.; Pedersen, T. *J. Mol. Struct.* **1980**, *65*, 43. (c) Carreira, L. A.; Towns, T. G. *J. Mol. Struct.* **1977**, *41*, 1.

(24) Sunner, B.; Piette, L. H.; Schneider, W. G. *Can. J. Chem.* **1960**, *38*, 681. Kamei, J. *Bull. Chem. Soc. Jpn.* **1968**, *41*, 2269. Drakenberg, T.; Forsen, S. *J. Phys. Chem.* **1974**, *74*, 1.

(25) Farminer, A. R.; Webb, G. A. *J. Mol. Struct.* **1975**, *27*, 417.

(26) Kintzinger, J. P.; Lehn, J. M.; Williams, R. L. *Mol. Phys.* **1969**, *17*, 135.

(27) Tannenbaum, E.; Myers, R. J.; Gwinn, W. D. *J. Chem. Phys.* **1956**, *25*, 42.

(19) Liebman, J. F. In *Molecular Structure and Energetics*; Liebman, J. F., Greenberg, A., Eds.; VCH: Deerfield Beach, Florida, Vol. 3, p 267ff, especially pp 319–320.

(20) Bader, R. F. W.; Nguyen-Dang, T. T. *Adv. Quantum Chem.* **1981**, *14*, 63.

(21) McClellan, A. L. *Tables of Experimental Dipole Moments*; W. H. Freeman: San Francisco, 1963.

**Table IV.** Linear Free Energy Parameters, Nitrogen Configuration (pl = planar, py = pyramidal), and Inversion Barrier (in kcal/mol) for X-NH<sub>2</sub> [Experimental Observations Are Quoted for the Latter Two Quantities, Except for Acetylenamine and Nitrosoamine; In These Cases, High-Quality Calculations Are Available]

X	$R^a$	$\sigma_R^b$	$\sigma_R^{-b}$	$\sigma_r^c$	geom	barrier	ref
HC≡C	-0.088	-0.04			py	1.7	<i>d</i>
H <sub>2</sub> C=CH		-0.15			py	-1.1-2	<i>e</i>
phenyl		-0.11			py	1.5	<i>f</i>
CH <sub>3</sub>	-0.141	-0.162		-0.08	py	4.9	<i>g</i>
H	0.0	0.0		0.0	py	5.8	<i>h</i>
CN	0.184	0.08	0.26	0.10	py	1.4	<i>i</i>
NO <sub>2</sub>	0.155	0.10	0.37	0.18	py	2.7	<i>j</i>
NO				0.26	py	0.1?	<i>k</i>
H <sub>3</sub> CCO	0.202	0.20		0.17	pl	0.0	<i>l</i>
HCO		0.15	0.53	0.19	pl	0.0	<i>l</i>

<sup>a</sup>Swain, C. G.; Lupton, E. C., Jr. *J. Am. Chem. Soc.* **1968**, *90*, 4328.  
<sup>b</sup>Charton, M. *Prog. Phys. Org. Chem.* **1981**, *13*, 119. <sup>c</sup>Taft, R. W.;  
 Topsom, R. D. *Prog. Phys. Org. Chem.* **1987**, *16*, 1. <sup>d</sup>Molecule has  
 been recently observed: Wentrup, C.; Breiht, H.; Lorencak, P.; Vo-  
 gelbacher, U. J.; Winter, H.-W.; Maquesttian, A.; Flammang, R. *J.*  
*Am. Chem. Soc.* **1988**, *110*, 1337. Previous high-quality calculations  
 predict pyramidal amine: Brown, R. D.; Rice, E. H. N.; Rodler, M.  
*Chem. Phys.* **1985**, *99*, 347 and ref 10. <sup>e</sup>Hamada, Y.; Sato, N.; Tsu-  
 boi, M. *J. Mol. Spectrosc.* **1987**, *124*, 172. Brown, R. D.; Godfrey, P.  
 D.; Kleiboemer, B. *Ibid.* **1987**, *124*, 21. <sup>f</sup>Kydd, R. S.; Krueger, P. J.  
*Chem. Phys. Lett.* **1977**, *49*, 539. <sup>g</sup>Reference 16. <sup>h</sup>Reference 15.  
<sup>i</sup>Brown, R. D.; Godfrey, P. D.; Kleiboemer, B. *J. Mol. Struct.* **1985**,  
*114*, 257. <sup>j</sup>Reference 3. <sup>k</sup>Harrison, J. A.; MacLagan, R. G. A. R.;  
 Whyte, A. R. *Chem. Phys. Lett.* **1986**, *130*, 98. <sup>l</sup>Hansen, E. L.; Lar-  
 sen, N. W.; Nicolaisen, F. M. *Chem. Phys. Lett.* **1980**, *69*, 327.

rameters characterizing resonance interactions. Indeed, barriers to pyramidal inversion are correlated with  $\sigma^-$  for meta- and para-substituted *N*-phenyl-2,2-dimethylaziridines.<sup>28</sup> For an NH<sub>2</sub> group directly substituted without an insulating phenylene group, highly accurate quantitative information is difficult to obtain on the barrier size or exact geometry. Nevertheless, qualitative trends might be examined. Table IV shows several types of linear free energy parameters and the preferred geometries of X-NH<sub>2</sub> compounds. The linear free energy parameters are generally said to be characteristic of resonance effects—just the sort of effect operating in II. Indeed, the largest  $R$ ,  $\sigma_R$ , and  $\sigma_R^-$  values occur for CH<sub>3</sub>CO as well as HCO, and these amides are found to be planar. In contrast,  $\sigma_r$  values do not indicate why nitramide is pyramidal while formamide is planar. Even more noticeable is

(28) Andose, J. D.; Lehn, J.-M.; Mislow, K.; Wagner, J. *J. Am. Chem. Soc.* **1970**, *92*, 4050.

the large  $\sigma_r$  value for NO, while nitrosoamine is nonplanar, although apparently just barely.

More significant, however, is the lack of even qualitative correlation between life parameters and the size of the inversion barrier. Both electron-donating and electron-withdrawing substituents lead to smaller barriers than in ammonia. This observation is consistent with  $\pi$  polarizability playing a role in determining these barriers. Nevertheless, substituents with extremely strong  $\pi$  donor or acceptor properties, such as anions or cations, are expected to lead to pyramidal or planar amines, respectively. What these observations suggest is that  $\pi$  resonance effects are not extensively involved in the ground-state descriptions of the substituted amines shown in Table IV. The calculated data presented in this paper show, in addition, that the geometry, total charge distribution, and thermodynamic stability of nitramide are not explained by invoking resonance forms such as II for nitramide.

We thus conclude that substituents with very strong  $\pi$  donor or acceptor properties may determine the amine configuration through resonance interaction, but the role of resonance for many common substituents with less extreme  $\pi$  properties is oftentimes not great and other factors may dominate. In addition, some molecular properties are more responsive than others to the involvement of valence bond structures such as II, depending upon their sensitivity to the local electron density. Murdoch and Magnoli showed that energy additivity, indicating a lack of resonance effects, does not require even nearly unperturbed electron density distributions about the functional groups involved.<sup>29</sup> The perturbations tend to cancel one another out. Thus,  $\pi$  charges at the para carbon in substituted benzenes can be correlated with <sup>13</sup>C chemical shifts, but total charges are not.<sup>30</sup> Similarly, it is difficult to detect this involvement of charge separated resonance structures in determining the geometries of substituted benzenes.<sup>31</sup> Because transition states, charged and open-shell species, and excited states are of a high energy, their description necessarily differs from that of a ground state for a closed-shell, neutral molecule. Involvement of such structures may be correspondingly larger in higher energy states. Charge-separated resonance structures must, however, be used with caution in interpreting the properties of ground-state, closed-shell, neutral molecules.

Registry No. Nitramide, 7782-94-7.

(29) Murdoch, J. R.; Magnoli, D. E. *J. Am. Chem. Soc.* **1982**, *104*, 2782.  
 (30) Hehre, W. J.; Taft, R. W.; Topsom, R. D. *Prog. Phys. Org. Chem.* **1976**, *12*, 159.  
 (31) (a) Bock, C. W.; Trachtman, M.; George, P. *J. Mol. Struct. (Theochem.)* **1985**, *122*, 155. (b) George, P.; Bock, C. W.; Trachtman, M. *J. Mol. Struct. (Theochem.)* **1986**, *137*, 387. (c) Domenicano, A.; Murray-Rust, P. *Tetrahedron Lett.* **1979**, *24*, 2283.